

# Selective degradation of PL2L60 by metabolic stresses-induced autophagy suppresses multi-cancer growth

LEI SUN<sup>1,2</sup>, FU HUI<sup>2</sup>, GAO-YAN TANG<sup>2</sup>, HAI-LIAN SHEN<sup>3</sup>, XUE-LEI CAO<sup>4</sup>, JIAN-XIN GAO<sup>1</sup> and LIN-FENG LI<sup>1</sup>

<sup>1</sup>The State Key Laboratory of Oncogenes and Related Genes, and The Laboratory of Tumorigenesis and Immunity, Renji-Med X Clinical Stem Cell Research Center, Ren Ji Hospital, School of Medicine, Shanghai Jiao Tong University, PuDong, Shanghai 200127; <sup>2</sup>Department of Oncology, First Affiliated Hospital of Weifang Medical University, Weifang, Shandong 261000, P.R. China; <sup>3</sup>Sam and Ann Barshop Institute for Longevity of Aging Studies, University of Texas Health Science Center at San Antonio, San Antonio, TX 78292, USA; <sup>4</sup>Department of Clinical Laboratory, Qi Lu Hospital of Shandong University, Jinan, Shandong 250012, P.R. China

Received June 22, 2023; Accepted November 8, 2023

DOI: 10.3892/or.2024.8700

**Abstract.** It has been reported that PL2L60 proteins, a product of *PIWIL2* gene which might be activated by an intragenic promoter, could mediate a common pathway specifically for tumorigenesis. In the present study, it was further identified by using western blot assay that the PL2L60 proteins could be degraded in cancer cells through a mechanism of selective autophagy in response to oxidative stress. The PL2L60 was downregulated in various types of cancer cells under the hypoxic condition independently of HIF-1 $\alpha$ , resulting in apoptosis of cancer cells. Inhibition of autophagy by small interfering RNA targeting of either Beclin-1 (*BECN1*) or Atg5 resulted in restoration of PL2L60 expression in hypoxic cancer cell. The hypoxic degradation of PL2L60 was also blocked by the attenuation of the autophagosome membrane protein Atg8/microtubule-associated protein 1 light chain 3 (LC3) or autophagy cargo protein p62 expression. Surprisingly, Immunofluorescence analysis demonstrated that LC3 could be directly bound to PL2L60 and was required for the transport of PL2L60 from the nucleus to the cytoplasm for lysosomal

flux under basal or activated autophagy in cancer cells. Moreover, flow cytometric analysis displayed that knocking down of PL2L60 mRNA but not *PIWIL2* mRNA effectively inhibited cancer cell proliferation and promoted apoptosis of cancer cells. The similar results were obtained from *in vivo* tumorigenic experiment, in which PL2L60 downregulation in necroptosis areas was confirmed by immunohistochemistry. These results suggested that various cancer could be suppressed by promoting autophagy. The present study revealed a key role of autophagic degradation of PL2L60 in hypoxia-induced cancer cell death, which could be used as a novel therapeutic target of cancer.

## Introduction

Piwi-like RNA-mediated gene silencing 2 (*PIWIL2*) gene has been identified as a common mediator for the development of various types of cancers. It is activated by an intragenic promoter, resulting in a tumorigenic variant called *PIWIL2*-like protein 60 (PL2L60) (1-6). Piwi proteins, a subfamily of the Argonaute family, are associated with Piwi-interacting RNAs (piRNAs), a class of small non-coding RNAs (snRNAs) and are involved in the biogenesis, transport, and use of these snRNAs (7,8). The *Piwil2* gene, alias *Mili* in mouse or *Hili* in human, is inclined to produce a full length of *Piwil2*, which binds piRNAs to form pi-ribonucleoproteins (piRNPs) and initiates transposon silencing in the germ line (9-11). In adult cells, *PIWIL2* gene is usually silenced but activated upon DNA damage, mediating DNA repair or promoting cell apoptosis in case that DNA repair is failed (12).

Alternative gene splicing provides a means by which cells generate proteins with different properties from a single mRNA precursor (13,14). The alternative splicing (AS) produces transcript 'isoforms' for most human genes, providing functional diversity at the level of enzymatic activities and subcellular localizations, as well as protein-protein, protein-DNA and protein-ligand physical interactions (15,16). However, it has been recently found that an isoform of *PIWIL2* gene is not generated from AS of mRNA but derived from alternative activation of an intragenic promoter (ITP), resulting in a truncated,

---

*Correspondence to:* Dr Lin-Feng Li or Professor Jian-Xin Gao, The State Key Laboratory of Oncogenes and Related Genes, and The Laboratory of Tumorigenesis and Immunity, Renji-Med X Clinical Stem Cell Research Center, Ren Ji Hospital, School of Medicine, Shanghai Jiao Tong University, 160 PuJian Road, PuDong, Shanghai 200127, P.R. China  
E-mail: lilinfeng@renji.com  
E-mail: jianxingao@sjtu.edu.cn; 15618820486@163.com

**Abbreviations:** AS, alternative splicing; PL2L60, *Piwil2*-like 60 kDa protein; piRNA, piwi-interacting RNA; HIF-1 $\alpha$ , hypoxia-inducible factor 1 alpha subunit; LC3, microtubule-associated protein 1 light chain 3 (MAP1LC3); ATG, autophagy-related gene; siRNA, small interfering RNA; PCD, programmed cell death

**Key words:** PL2L60, autophagy, autophagic cell death, hypoxia, cancer

alienated product PL2L60 (2,4,5). While a full length of Piwil2 protein may serve as a tumor barrier (12), PL2L60 depleted of Piwil2 exon 1-5 is preferentially expressed in various types of human cancer cells, promoting tumorigenesis and tumor growth (4,12). However, little is known for the mechanisms that regulate PL2L60 protein expression in cancer cells.

Hypoxia is an intrinsic stress occurring within the tumor microenvironment due to the rapid growth of cancer cells, poorly formed neoangiogenic blood vessels, or even radiotherapy and chemotherapy-induced ischemia (17,18). The cells deprived of oxygen will initially employ adaptive and survival strategies (19), but cell death will eventually occur if hypoxia is sustained (20). The precise mechanisms of hypoxia-induced cell death remain unclear as apoptosis, necrosis and autophagy have all been reported in response to hypoxic stress (21). Since PL2L60 plays a critical role for the survival and proliferation of cancer cells, it was hypothesized that hypoxia-induced cell death might be associated with degradation of PL2L60 proteins mediated by autophagy.

Autophagy is a catabolic process that maintains cellular homeostasis through the degradation of cellular constituents and the generation of basic building blocks for the synthesis of new macromolecules (22). Autophagy is best characterized to be induced under stressful conditions, such as organelle damage, hypoxia or nutrient deprivation, and is followed by the elongation of the autophagosome membrane around its cargo (23). The ubiquitin-like protein Atg8, which is conjugated to phosphatidylethanolamine (PE), associates with outer and inner membranes of autophagic structures (24). Autophagosomes eventually fuse with lysosomes to degrade their content. The autophagic process requires a set of evolutionarily conserved proteins, most of which are known as autophagy-related (ATG) proteins, functioning at different phases of autophagy formation (24). Initially described as a key survival feature for cancer cells, autophagy has raised great attention for its potential ability to promote cell death (25,26). While autophagosomes were initially identified in dying cells, a phenomenon that led to the term 'autophagic cell death' to describe a cell death mode is distinct from apoptosis (26). Therefore, autophagy plays a critical role in maintaining cellular homeostasis and is regarded as a double-edged sword. While autophagy primarily acts in a cyto-protective manner, the dysregulated states could result in compromised cell function and even death (19,20,25-28). Previously, it was verified by the authors that severe hypoxia could induce autophagic cell death (28). Since PL2L60 is associated with tumor cell proliferation (2), it is possible that decreased PL2L60 might play a key role in the hypoxia-induced autophagic cell death.

In the present study, the involvement of PL2L60 in hypoxia-induced autophagic cancer cell death was investigated using *in vitro* and *in vivo* models.

## Materials and methods

**Cell lines and reagents.** Human cancer cell lines including breast [MDA-MB-231 (cat. no. HTB-26<sup>TM</sup>), MDA-MB-468 (cat. no. HTB-132<sup>TM</sup>), MCF-7 (cat. no. HTB-22<sup>TM</sup>), T-47D (cat. no. HTB-133<sup>TM</sup>) and SKBR3 (cat. no. HTB-30<sup>TM</sup>)], lung [A549 (cat. no. CCL-185<sup>TM</sup>)], colon [HCT116 (cat. no. CCL-247<sup>TM</sup>)], cervix [HeLa (cat. no. CCL-2<sup>TM</sup>)], prostate [PC-3 (cat. no. CRL-1435<sup>TM</sup>)]

and liver [HepG2 (cat. no. HB-8065<sup>TM</sup>)] were obtained from the American Type Culture Collection. The cells were cultured in Dulbecco's modified Eagle medium (Gibco; Thermo Fisher Scientific, Inc.) supplemented with 10% fetal bovine serum and 100 U/ml penicillin-streptomycin (Gibco; Thermo Fisher Scientific, Inc.). The cells were maintained in a humidified incubator containing 5% CO<sub>2</sub> and air at 37°C. Cobaltic chloride (CoCl<sub>2</sub>; cat. no. C8661; Sigma-Aldrich; Merck KGaA) was dissolved in water to create 40 mmol/l stock solutions and stored at -20°C. Rapamycin (cat. no. HY-10219; MedChemExpress) was dissolved in DMSO to create 10 mmol/l stock solutions and stored at -20°C.

**Transfection of small interfering RNA (siRNA).** Non-targeting control siRNA and targeting siRNA were purchased from Shanghai GenePharma Co., Ltd. The siRNA sequences were as follows: *BECN1*: 5'-UGUGAAUGGAAUGAGAUUATT-3'; *ATG5*: 5'-CCAUCAUCGGAAACUCAUTT-3'; *Piwil2-siE5* (*Piwil2* full length): 5'-GCCTGTTAAGCTTCAACAATT-3'; *Piwil2-siE21* (*PL2L60*): 5'-CUAUGAGAUUCCUCAACUACA GAAG-3'; *HIF-1α*: 5'-GGAAAUGAGAGAAAUGCUUTT-3'; microtubule-associated protein 1 light chain 3 (*LC3*): 5'-CUC CCUAAGAGGAUCUUUATT-3'; *p62*: 5'-GGAGUCGGAUAA CUGUUCATT-3'; and negative control: 5'-UUCUCCGAA CGUGUCACGUTT-3'. After breast cancer (MDA-MB-231), lung cancer (A549), or cervix cancer (HeLa) cancer cells being seeded at 2.0-2.4x10<sup>5</sup> per well in six-well plates overnight, siRNA duplexes (50 pmol) were transfected into the target cell populations using Lipofectamine<sup>®</sup> 2000 Reagent (Invitrogen; Thermo Fisher Scientific, Inc.) for 6 h according to the manufacturer instructions. After 48 h of transfection, cells were used for subsequent experiments.

**Cell viability assay.** The siRNA transfected cells (3x10<sup>3</sup> cells/well) were initially seeded in 96-well flat-bottomed plates in quintuplicate for another 24 h. Viable proliferating cells were detected using the Cell Counting Kit-8 (Dojindo Laboratories, Inc.), according to manufacturer's instruction. CCK-8 reaction mixture for each well in one 96-wells plate consisted of 100 μl DMEM and 10 μl CCK-8 reagent and was incubated for 30 min at 37°C. The OD value for each well was measured on a Synergy HT microplate reader (BioTek Instruments, Inc.) at 450 nm wavelength. Cell viability was calculated with the following formula: Inhibition percentage (%)=(control siRNA transfected sample-targeted siRNA transfected sample)/(control siRNA transfected sample) x100%.

**Apoptosis assays.** Apoptosis was detected by flow cytometric analysis following PI/Annexin V double staining (cat. no. 640932; Biolegend, Inc.). The ratio of cells in early apoptosis and late apoptosis were calculated, and statistical analysis of the data was performed. All flow cytometric analysis was performed on a BD C6 flow cytometer (BD Biosciences). Data were analyzed using FlowJo software version 7.6.1 (Tree Star Inc.).

**Western blot analysis.** Cells were lysed in pre-cold radio-immunoprecipitation (RIPA) assay buffer (Thermo Fisher Scientific, Inc.) containing 1X protease inhibitor cocktail (Roche Diagnostics) on ice. Protein concentration in the soluble lysates was quantified using a bicinchoninic acid (BCA) protein assay. Protein samples (20 μg) were separated

by 8-12% sodium dodecyl sulfate-polyacrylamide gel electrophoresis (SDS-PAGE) and transferred to polyvinylidene fluoride membranes (Millipore Sigma). Membranes were blocked with 5% non-fat dry milk in TBST at room temperature for 1 h, followed by overnight incubation with primary antibodies at 4°C in EZ-Buffers N 1X BLOCK BSA in TBS (cat. no. C500036; Sangon Biotech Co., Ltd.). Western blots were performed using the following primary antibodies: anti-HIF-1 $\alpha$  (1:500; cat. no. YM0333; Immunoway Biotechnology Company), anti-LC3B (1:1,000; cat. no. 3868; Cell Signaling Technology, Inc.), anti-Beclin-1 (1:1,000; cat. no. 3495; Cell Signaling Technology, Inc.), anti-ATG5 (1:1,000; cat. no. 12994; Cell Signaling Technology, Inc.), anti-p62 (1:2,000; cat. no. 18420-1-AP; Proteintech Group, Inc.), anti-Piwil2/PL2L60 (1:1,000; generated in the authors' lab) and anti- $\beta$ -actin (1:3,000; cat. no. MA5-11869; Invitrogen, Thermo Fisher Scientific, Inc.). PVDF membranes were washed and incubated with HRP-conjugated rabbit (1:2,000; cat. no. 7074; Cell Signaling Technology, Inc.) or mouse (1:3,000; cat. no. 7076; Cell Signaling Technology, Inc.) secondary antibodies for 1 h at room temperature. The membranes were visualized with Super Signal<sup>®</sup> West Pico Chemiluminescent Substrate kit (Thermo Fisher Scientific, Inc.), and image acquisition was made with the ChemiDox<sup>™</sup> XRS<sup>+</sup> system. The differences in protein expression among various treatments were determined using the image analysis software ImageJ software version 1.8.0 (National Institutes of Health), using  $\beta$ -actin as a loading control.

**Nuclear and cytoplasmic fractionations.** Nuclear and cytoplasmic extracts were prepared using NE-PER Nuclear and Cytoplasmic Extraction Reagents (cat. no. 78833; Pierce, Thermo Fisher Scientific, Inc.). The quality of nuclear and cytoplasmic extracts was verified by immunoblotting with protein differentially enriched in the nucleus or the cytoplasm ( $\beta$ -actin).

**Lentiviral transduction.** Lentiviral packaging plasmids psPAX2 and pMD2.VSV-G were co-transfected with the puromycin resistant GFP-LC3 construct (ChenDu Transvector Biotechnology Co., Ltd.) into 293T cells for virus production at 37°C under 5% CO<sub>2</sub>. Briefly, 293T cells were plated in 10-cm dishes and transfected with GFP-LC3 construct, psPAX2 and pMD2.VSV-G at a ratio of 4:3:1. Virus-containing media were collected 72 h post-transfection and used to infect MDA-MB-231 cells in the presence of 5  $\mu$ g/ml Polybrene. After 24 h of infection, the infected cells were selected with puromycin (5  $\mu$ g/ml) for one week to establish stable GFP-LC3 expression cells. The cells were further passaged for 1-2 generations before experiments.

**Immunofluorescence and imaging.** MDA-MB-231 cells stably transfected by LC3-GFP at 50% confluence were fixed with 4% paraformaldehyde (Beijing Dingguo Changsheng Biotechnology Co., Ltd.) for 15 min at room temperature followed by permeabilization with 0.25% (w/v) Triton X-100 (MilliporeSigma). Cells were then blocked for 1 h in 3% BSA at room temperature and incubated overnight with primary antibody (Piwil2; 1:50) at 4°C. Then cells were incubated with secondary antibodies conjugated with Alexa Fluor<sup>®</sup> 555

conjugate (Thermo Fisher Scientific, Inc.) at room temperature for 1 h followed by three washes with PBS. After washing, the slides were counterstained with 4'6'-diamidino-2-phenylindole dihydrochloride (DAPI; 2  $\mu$ g/ml) (Sigma-Aldrich; Merck KGaA) for 5 min. Images were acquired by using 20X Ti-S fluorescence scanning microscope (Nikon Corporation) objective.

**Animal experiments.** Nude mice (total number, 16; 50% male and 50% female; weight, ~23 g) were obtained from SLACCAS (Shanghai Laboratory Animal Center). Mice were bred in the authors' animal pathogen-free facility (SPF) and maintained under standard conditions according to the institutional guidelines of Renji Hospital animal care and ethics review committee (Shanghai, China). The temperature of SPF animal room was maintained at 20-26°C (maximum temperature difference <4°C), the relative humidity at 40-70%, the noise was kept at <60 decibels, the ammonia concentration <14 mg/m<sup>3</sup>, the ventilation >15 times/h, the light/dark cycle condition was 12/12-h, and the bottom of the cage was placed with autoclave corn cob as bedding material. The feeding density was  $\leq$  5 animals per cage. The drinking water was sterilized by the animal drinking water system. The feed was special sterile pellets for mice, which were checked twice a day. Feed, drinking water and cage were changed once a week. Nude mice were used at age of 6-8 week. All *in vivo* experiments were approved by the institutional guidelines of Renji Hospital animal care and ethics review committee. 1x10<sup>7</sup> breast cancer MDA-MB-231 or cervical cancer HeLa cells were suspended in 200  $\mu$ l of PBS and then subcutaneously injected into nude mice, and the mice were monitored for up to 4 weeks. Tumor volume was measured using a caliper every three days and calculated using the formula: V (mm<sup>3</sup>)=0.5x length x width<sup>2</sup>. Afterwards, the mice were humanely euthanized via CO<sub>2</sub> asphyxiation with a flow rate displacing 30% of the chamber volume per min when the tumor diameter reached 2 cm, and each tumor was confirmed by routine H&E staining of paraffin sections.

**Immunohistochemistry (IHC).** Paraffin-embedded tissues were sectioned (5  $\mu$ m thickness) and stained with H&E or stored for further paraffin or fluorescence IHC. Sections were incubated with target retrieval solution (Dako; Agilent Technologies, Inc.) in a steamer for 45 min followed by 3% hydrogen peroxide solution for 10 min and protein block (Dako; Agilent Technologies, Inc.) for 20 min at room temperature. Sections were incubated overnight in a humid chamber at 4°C with the following antibodies (all diluted at a ratio of 1:500) against: HIF-1 $\alpha$  (cat. no. ab82832; Abcam), LC3, p62, Ki-67 (cat. no. 9027; Cell Signaling Technology, Inc.), cleaved-caspase 3 (cat. no. 9664; Cell Signaling Technology, Inc.) and PL2L60 (generated in the authors' lab) followed by biotinylated secondary antibody (1:1,000; Vector Laboratories, Inc.) for 30 min and ABC reagent for 30 min. Immunocomplexes of horseradish peroxidase were visualized by DAB reaction (Dako; Agilent Technologies, Inc.), and sections were counterstained with haematoxylin before mounting. Micrographs of stained sections were captured using a Leica DMIL LED microscope with an Amscope camera and acquisition software.

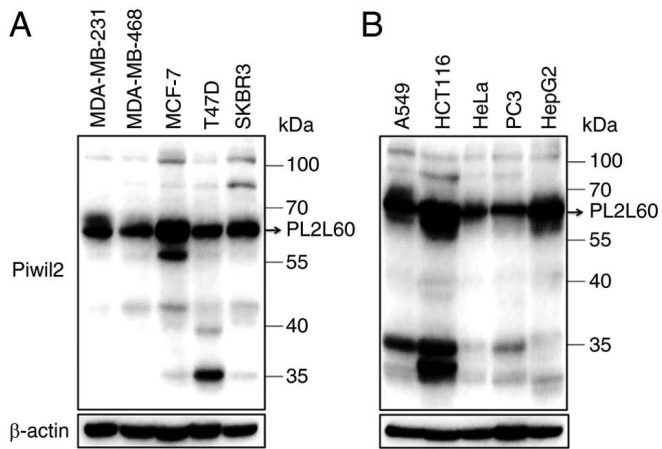


Figure 1. PL2L60 rather than PIWIL2 is predominantly expressed in various types of cancer cells. (A and B) Protein levels of Piwil2 and PL2L60 (60 kDa) in (A) five breast cancer cell lines and (B) lung (A549), colon (HCT116), cervical (HeLa), prostate (PC3) and liver (HepG2) cancer cell lines were measured by western blot analysis. Piwil2 full length: 110 kDa; PL2L60: 60 kDa. PL2L60, Piwil2-like 60 kDa protein; PIWIL2, Piwi-like RNA-mediated gene silencing 2.

**Statistical analysis.** All data are expressed as the mean  $\pm$  standard deviation (SD) and are representative of triplicate samples. Statistical analysis was performed using GraphPad Prism 5 software (Dotmatics). Statistical comparisons were made by using two-tailed unpaired Student t-tests.  $P \leq 0.05$  was considered to indicate a statistically significant difference.

## Results

*PL2L60 is predominantly expressed in various types of cancer cells but decreased upon oxygen deprivation.* It has been reported by the authors that PL2L60 protein, a variant of PIWIL2, which is alternatively activated by its ITP, mediates tumorigenesis and tumor growth (2,4). The PL2L60 expression is significantly inhibited by siRNA against exon 21 (siRNA-E21) but not by siRNA against exon 7 (siRNA-E7) of *PIWIL2* gene (4,5). The expression levels of PIWIL2 and PL2L60 were therefore further analyzed in a number of human cancer cell lines. As demonstrated in Fig. 1A and B, almost all the tumor cell lines examined expressed PL2L60 in a level markedly higher than PIWIL2. These lines included cancer cells from breast cancer (MDA-MB-231, MDA-MB-468, MCF-7, T-47D and SKBR3), lung cancer (A549), colon cancer (HCT116), cervix cancer (HeLa), prostate cancer (PC3) and liver cancer (HepG2). By contrast, all lines expressed little full length of PIWIL2, consistently with the authors' previous observation (2). Since the growth rate of tumor is always associated with blood or oxygen supply and nutrition supply, it was investigated whether PL2L60 expression was affected by low oxygen availability. A total of five different breast cancer cell lines (MDA-MB-231, MDA-MB-468, MCF-7, T-47D and SKBR3) were exposed to normoxia (21%  $O_2$ ) and hypoxia (1%  $O_2$ ) for 24 h, respectively, followed by PL2L60 protein expression measurement by western blot analysis. After 24 h hypoxic exposure, the PL2L60 protein level was markedly reduced (Fig. 2A). To determine whether the result was universal or restricted to human breast cancer

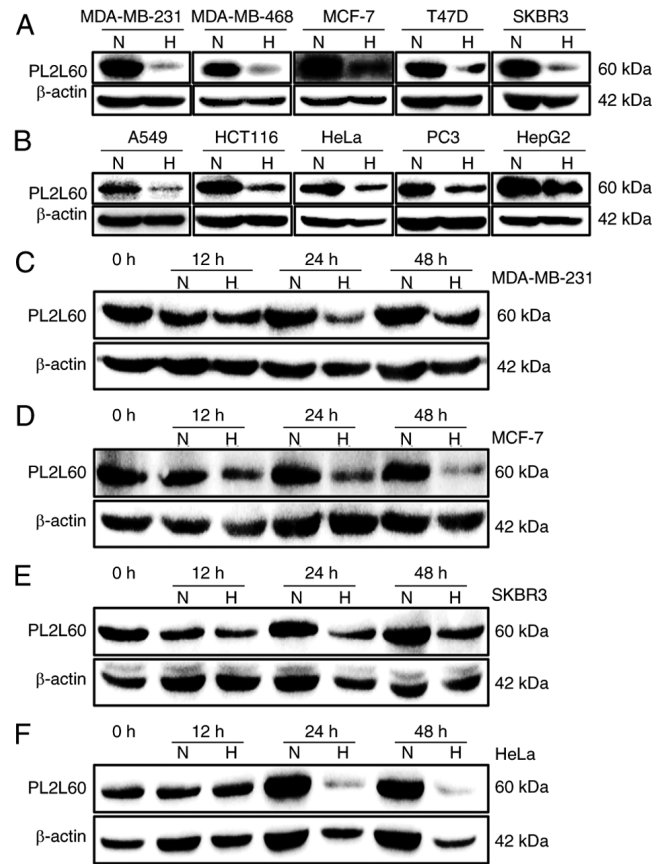
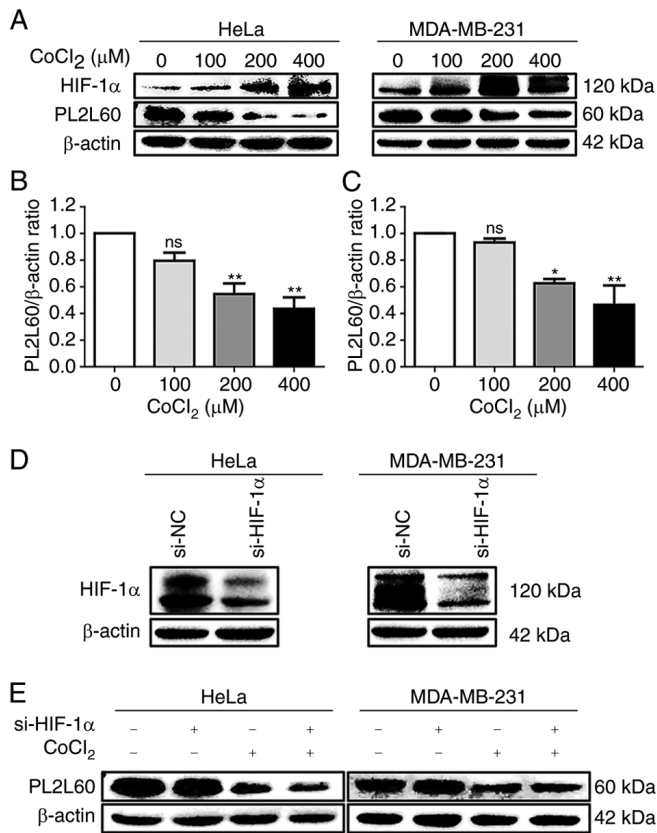


Figure 2. Hypoxia suppresses PL2L60 protein expression in various types of cancer cells. (A and B) The effects of oxygen levels on PL2L60 expression in various types of cancer cell lines grown in normoxia (N; 21%  $O_2$ ) or hypoxia (H; 1%  $O_2$ ) for 24 h. The cells were harvested and measured for PL2L60 protein levels by western blotting. (A) Breast cancer cells including MDA-MB-231, MDA-MB-468, MCF-7, T-47D and SKBR3. (B) Cancer cell lines from various types of tissues including lung (A549), colon (HCT116), cervix (HeLa), prostate (PC3) and liver (HepG2). (C-F) Kinetics of hypoxia-induced decreasing PL2L60 expression in various types of cancer cell lines, including (C) MDA-MB-231, (D) MCF-7, (E) SKBR3 and (F) HeLa, which were cultured in hypoxia (H; 1%  $O_2$ ) for 0, 12, 24 and 48 h. It should be noted that PL2L60 was consistently decreased at 24 h under hypoxia. PL2L60, Piwil2-like 60 kDa protein.

cells, human cancer cell lines from other tissues were also examined, including lung (A549), colon (HCT116), cervix (HeLa), prostate (PC3) and liver (HepG2). The same results were observed after these cell lines were exposed to normoxia or hypoxia for 24 h. As expected, PL2L60 was markedly reduced in the hypoxic cells compared with the cells exposed to normoxic condition (Fig. 2B). Kinetic analysis revealed that the levels of PL2L60 began to decrease but slightly as early as 12 h after exposure to hypoxia; at 24 and 48 h, the expression of PL2L60 was substantially reduced compared with the cells cultured under normoxic condition (Fig. 2C-F). These data revealed that PL2L60 expression in various types of cancer cells could be remarkably downregulated at late stage of hypoxic responses.

*Hypoxia-induced downregulation of PL2L60 is hypoxia-inducible factor 1 alpha subunit (HIF-1 $\alpha$ )-independent.* Since the evolutionarily conserved HIF transcriptional complex is rapidly activated when the  $O_2$  tension decreases (29) and the



**Figure 3.** Hypoxia-induced downregulation of PL2L60 in cancer cells is HIF-1 $\alpha$ -independent. (A-C) Dose-dependent expression of HIF-1 $\alpha$  and PL2L60 in cancer cells treated with cobalt chloride (CoCl<sub>2</sub>). (A) The HeLa cells and MDA-MB-231 cells were exposed CoCl<sub>2</sub> at the indicated concentration (0, 100, 200 and 400  $\mu$ M) for 24 h followed by western blot analysis of PL2L60, HIF-1 $\alpha$  and  $\beta$ -actin. (B and C) The band intensity of PL2L60 normalized by  $\beta$ -actin was decreased in a dose-dependent manner of CoCl<sub>2</sub>. (D and E) Knockdown of HIF-1 $\alpha$  had no effect on PL2L60 expression in the hypoxic cancer cells. (D) The HeLa and MDA-MB-231 cancer cells were transfected with HIF-1 $\alpha$  siRNA (si-HIF-1 $\alpha$ ) or control siRNA (si-NC) for 48 h, and HIF-1 $\alpha$  protein expression was analyzed by western blotting. (E) Then, HeLa and MDA-MB-231 cells transfected with siRNA negative control (si-NC) or HIF-1 $\alpha$  siRNA for 48 h were treated with CoCl<sub>2</sub> (400  $\mu$ M) or vehicles (PBS) for another 24 h. The results shown were a representative from 3 reproducible experiments. PL2L60, Piwil2-like 60 kDa protein; HIF-1 $\alpha$ , hypoxia-inducible factor 1 alpha subunit; si-, small interfering; NC, negative control; ns, no significance. \*P<0.05 and \*\*P<0.01.

HIF-1 $\alpha$  plays a key role in the regulation of oxygen homeostasis (30), it was investigated whether hypoxia-induced HIF-1 $\alpha$  was associated with PL2L60 downregulation in the cancer cells exposed to hypoxic condition. Cobalt chloride (CoCl<sub>2</sub>), which stabilizes HIF-1 $\alpha$  by inhibiting prolyl hydroxylases to induce cellular hypoxic responses *in vitro* (28,31) was used to treat breast cancer cell line MDA-MB-231 and cervical cancer cell line HeLa for 24 h in various concentrations (0, 100, 200 or 400  $\mu$ M). As demonstrated in Fig. 3, the expression of PL2L60 protein in both lines of cancer cells was inhibited by CoCl<sub>2</sub> in a dose-dependent manner (Fig. 3A-C), while HIF-1 $\alpha$  was remarkably increased. To determine whether the reduction of PL2L60 in the hypoxic cells was regulated by HIF-1 $\alpha$ , HIF-1 $\alpha$  expression was inhibited in HeLa and MDA-MB-231 cells by using siRNA (Fig. 3D). As a result, HIF-1 $\alpha$  siRNA did not have any significant effect on the PL2L60 protein expression either in the hypoxic or normoxic condition (Fig. 3E). Therefore, it

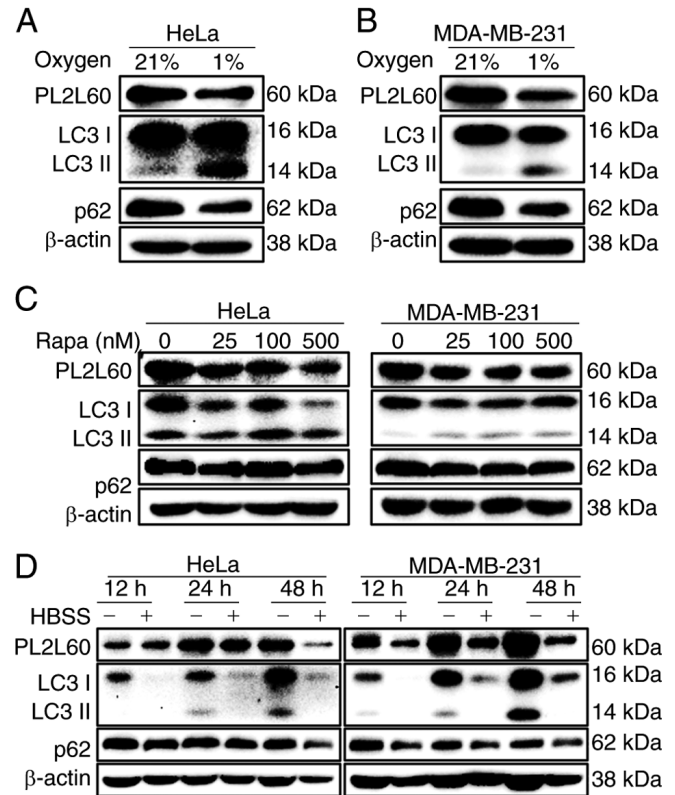


**Figure 4.** PL2L60 is synchronically downregulated with activation of autophagy induced by hypoxia, rapamycin or nutrient deprivation. (A and B) HeLa and MDA-MB-231 cancer cells were cultured under normoxia (N; 21% O<sub>2</sub>) or hypoxia (H; 1% O<sub>2</sub>) conditions for 24 h, (C) treated with rapamycin at the indicated concentrations (0, 25, 100 and 500 nM) for 24 h, or (D) deprived of serum from cultures for the indicated time intervals (12, 24 and 48 h). The expression levels of PL2L60, p62, LC3 and  $\beta$ -actin were assessed by immunoblot analysis. The results shown are representative of 3 reproducible experiments. PL2L60, Piwil2-like 60 kDa protein; LC3, microtubule-associated protein 1 light chain 3; HBSS, HBSS, Hank's Balanced Salt Solution.

was concluded that hypoxia-induced PL2L60 downregulation was independent of HIF-1 $\alpha$  expression in the hypoxic cancer cells.

*The downregulation of PL2L60 expression in the hypoxic cancer cells is associated with autophagy activated by hypoxia, rapamycin or nutrient starvation.* Since HIF-1 $\alpha$  had no effect on PL2L60 protein expression (Fig. 3), it was hypothesized that PL2L60 downregulation in the hypoxic cancer cells might be associated with autophagic activation, because the autophagy was activated in the human tumor cell lines when exposed *in vitro* to hypoxia and/or metabolic stress (28,32,33). Therefore, the association of LC3 expression with PL2L60 downregulation in the distressed cancer cells was examined, as autophagy was activated through recruiting LC3 (LC3-I) to autophagosome membranes, by which LC3-I is conjugated with PE to form punctate LC3-II (34). Under the hypoxic condition, HeLa and MDA-MB-231 cancer cells demonstrated decreased PL2L60 but increased LC3-II (Fig. 4A and B). Simultaneously, the level of p62 protein was also decreased (Fig. 4A and B), indicating an enhanced autophagic influx. The p62 is known to make a bridge between polyubiquitinated cargos and autophagosomes through binding, respectively, to

a ubiquitin-associated domain and a LC3-interacting region. The results suggested that decreased expression of PL2L60 in the hypoxic cancer cells was associated with autophagic activation. Consistently, PL2L60 expression was also decreased in both HeLa and MDA-MB-231 cancer cells treated by an autophagy activator rapamycin, an inhibitor of mTOR (Fig. 4C) or deprived of nutrients (Fig. 4D). Collectively, these data verified the hypothesis that HIF-1 $\alpha$ -independent downregulation of PL2L60 in the hypoxic cancer cells was associated with autophagic activation.

*Depletion of autophagic signaling components blocked PL2L60 degradation in hypoxic cancer cells.* To further confirm that autophagic activation was associated with the decreased expression of PL2L60 in the hypoxic cancer cells, the effects of depletion of autophagic components on PL2L60 expression were investigated. The autophagic process requires a series of evolutionarily conserved proteins, most of which are known as ATG proteins, functioning at different phases of autophagy formation. Beclin-1 binds to class III phosphatidylinositol 3-kinase (PIK3C3 or Vps34), which forms an initiation complex of autophagy and promotes autophagosomal membrane nucleation (35,36). Since autophagosomal elongation requires 2 ubiquitin like conjugation systems, ATG12-ATG5 and subsequent PE-conjugated form of LC3-II/ATG8-PE (37), Beclin-1, ATG5, p62 and LC3, respectively, were knocked down in cancer cells, using specific siRNA, and the levels of PL2L60 in these cells were examined. HeLa cells were transfected with *ATG5* or *Beclin-1* (*BECN1*)-specific siRNA for 48 h and subsequently exposed to 1% O<sub>2</sub> (hypoxia) or 21% O<sub>2</sub> (normoxia) for another 24 h. As expected, PL2L60 was not significantly decreased in the hypoxic HeLa cells when *ATG5* or *Beclin-1* was knocked down (Fig. 5A and B). Similar results were observed when LC3 or p62 was knocked out by siRNA in the hypoxic HeLa cells (Fig. 5C and D) and MDA-MB-231 cells (Fig. 5E and F). These results verified that PL2L60 downregulation in the hypoxic cancer cells is mediated by a mechanism of autophagic degradation.

*PL2L60 is predominantly expressed in the nucleus and degraded through forming a complex with autophagosome in the hypoxic cancer cell lines.* PIWI proteins are often detected in the perinuclear membrane-less organelle called the nuage (also known as Yb bodies, chromatoid bodies, pi-bodies and piP-bodies); therefore, the nuage is considered to be the center for piRNA biogenesis and piRNA-induced silencing complex (piRISC) formation (11,38,39). However, PL2L60 is a product of alienation-activated *PIWIL2* gene by its intragenic promoter (4), and thus is defective in N-terminal, affecting its subcellular localization and protein functions (40). Therefore, PL2L60 expression in the nucleus and cytoplasm was examined using immunofluorescent microscopy and western blotting. The results revealed that PL2L60 was predominantly expressed in the nucleus of cancer cells (Fig. 6A and B). Especially, dense nuage-like granules containing PL2L60 were clearly observed in the nuclei of cancer cells under normoxic condition. However, the granules turned out to be obscured in the hypoxic and nutrients-deprived cancer cells (Fig. 6A), in which autophagy

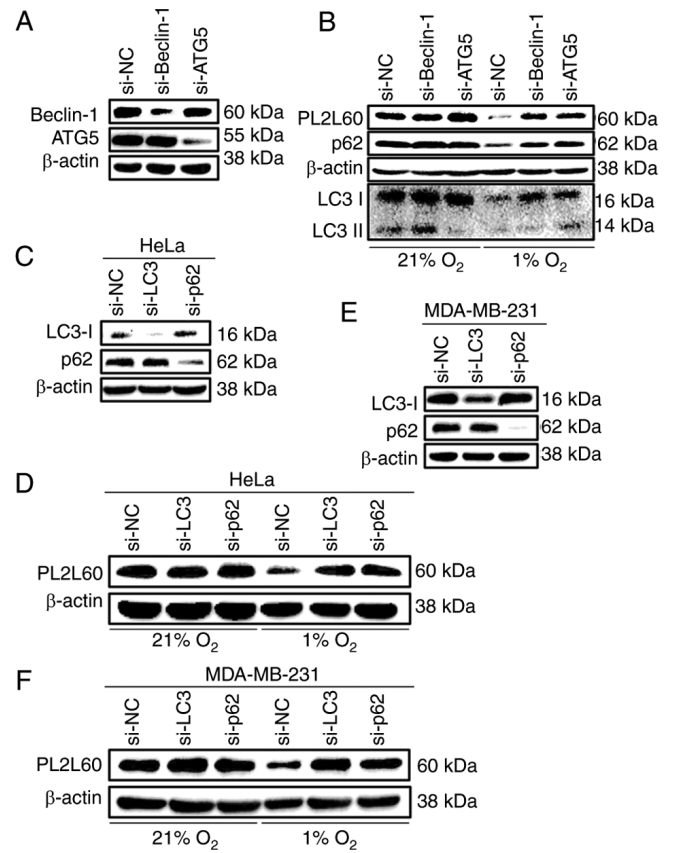


Figure 5. PL2L60 protein is degraded by selective autophagy in hypoxia. (A) HeLa cancer cells were transfected with Beclin-1 siRNA (si-Beclin-1), ATG5 siRNA (si-ATG5) or control negative control siRNA (si-NC) for 48 h. The levels of Beclin-1, ATG5 and  $\beta$ -actin were determined by immunoblotting. (B) HeLa cells were transfected with Beclin-1 siRNA (si-Beclin-1), ATG5 siRNA (si-ATG5) or control siRNA (si-NC) for 48 h and then exposed to 1% O<sub>2</sub> (hypoxia) or 21% O<sub>2</sub> (normoxia) for another 24 h. The cells were harvested and the levels of protein expression were measured by western blot analysis using antibodies against PL2L60, p62, LC3 and  $\beta$ -actin. (C) HeLa cancer cells and (E) MDA-MB-231 cancer cells were transfected with LC3 siRNA (si-LC3), p62 siRNA (si-p62) or negative control siRNA (si-NC) for 48 h. The levels of LC3, p62 and  $\beta$ -actin were determined by immunoblotting. (D) HeLa cancer cells and (F) MDA-MB-231 cancer cells were transfected with LC3 siRNA (si-LC3), p62 siRNA (si-p62) or control siRNA (si-NC) for 48 h and then exposed 1% O<sub>2</sub> (hypoxia) or 21% O<sub>2</sub> (normoxia) for another 24 h. The cells were harvested and the levels of protein expression were measured by western blot analysis using antibodies against PL2L60 and  $\beta$ -actin. PL2L60, Piwil2-like 60 kDa protein; siRNA, small interfering RNA; NC, negative control; LC3, microtubule-associated protein 1 light chain 3.

was activated (Fig. 5). In accordance with the observation, fractionation studies confirmed that PL2L60 was predominantly expressed in nucleus rather than in the cytoplasm (Fig. 6B). And the PL2L60 was significantly reduced in the nuclei of cancer cells under hypoxia for 24 h (Fig. 6B), suggesting that the nuclear PL2L60 might be degraded by hypoxia-induced autophagy. To confirm the hypothesis, breast cancer cell line MDA-MB-231 was stably transfected with GFP-LC3 and examined for the interaction between LC3 and PL2L60. As revealed in Fig. 7A, both GFP-LC3 and PL2L60 were mainly detected in the nuclei. And GFP-LC3 were fused or colocalized with PL2L60 nuage-like granules in the nucleus. Interestingly, some perinuclear areas in the cells under normoxic condition were rich of GFP-LC3 puncta but lacked of PL2L60 (Fig. 7B; arrow heads). Under normoxic

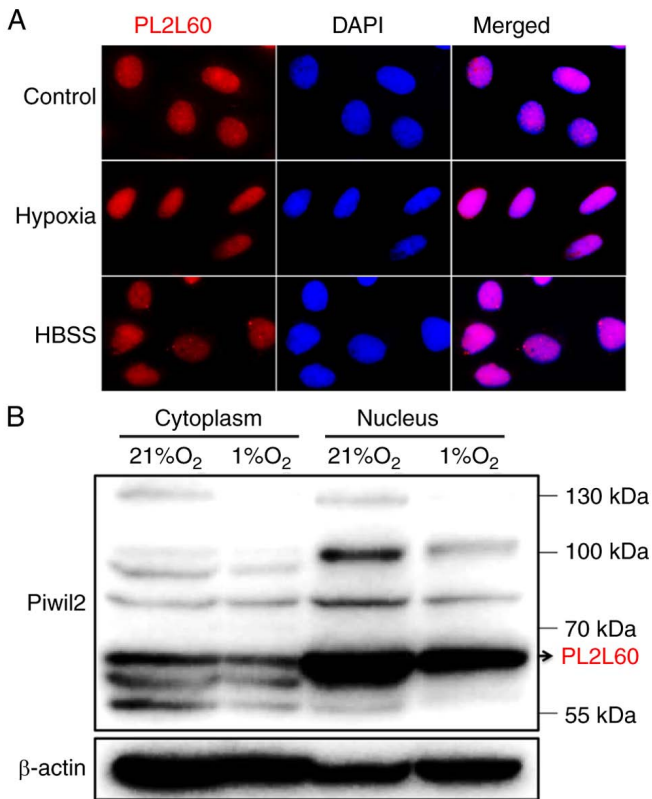


Figure 6. Sub-cell localization and expression of PL2L60 under hypoxia or nutrient deprivation in cancer cells. (A) Immunofluorescence analysis was performed to detect the localization and expression of PL2L60 in HeLa cervical cancer cells under hypoxia or nutrient deprivation for 24 h. DAPI-stained nuclei are shown in blue. (B) Western blotting results of the fractionation of cellular compartments from HeLa cervical cancer cells under 1% O<sub>2</sub> (hypoxia) or 21% O<sub>2</sub> (normoxia) for 24 h. PL2L60, Piiwil2-like 60 kDa protein.

condition, basal autophagy could still be activated in the cell cytoplasm where the autophagosomes containing LC3 puncta could be present (23). Therefore, the GFP-LC3 puncta lack of PL2L60 was likely perinuclear autophagosomes, in which PL2L60 might have been completely degraded (Fig. 7B; arrow heads). The results under basal autophagy condition were similar to the results in Fig. 6A where autophagy could be activated by hypoxia or nutrient starvation. The PL2L60 nuage-like granules in the cells under hypoxia condition were markedly less dense compared with those in the cells under normoxic condition (Fig. 6A). The results further conformed that PL2L60 can be degraded by autophagy in cancer cells.

**Silencing of PL2L60 induces apoptosis of cancer cells.** It has been previously reported by the authors that PL2L60 mediates tumorigenesis and silencing of PL2L60 using specific siRNA effectively inhibits tumor cell proliferation (4). This conclusion is supported by silencing of PL2L60 using siRNA E21 in cancer cells. MDA-MB-231, HeLa or A549 cancer cells were transfected with siRNA E21 at the indicated concentrations for 48 h and then assessed for the cell growth. As revealed in Fig. 8A and B, blocking PL2L60 expression potently inhibited growth of cancer cells including MDA-MB-231, HeLa and A549. This inhibition was obviously associated with increased apoptosis of cancer

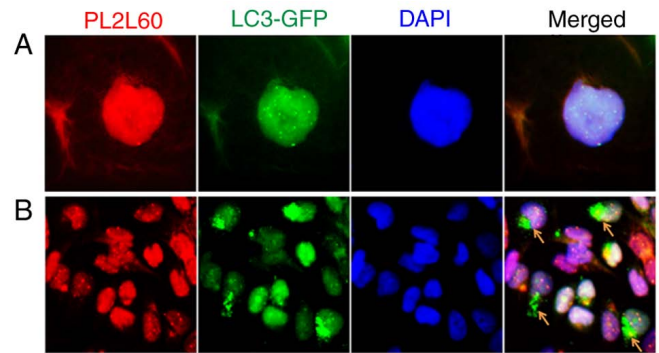
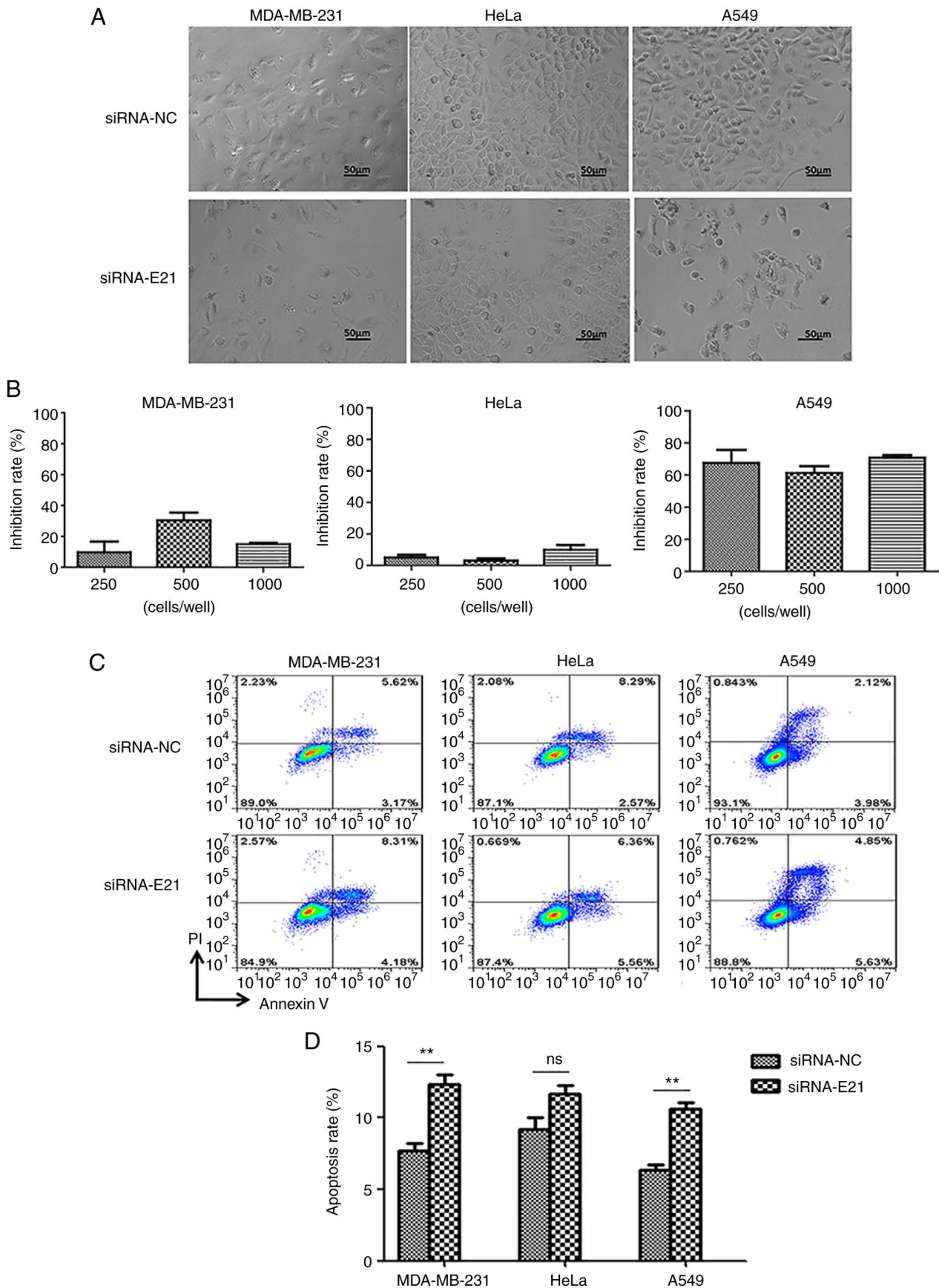


Figure 7. Interaction of PL2L60 with LC3 in the nucleus. Co-localization of endogenous PL2L60 with GFP-tagged LC3 (green) in stably transfected MDA-MB-231 cells, determined by immunostaining with anti-PL2L60 (red). DAPI, nuclei (blue). (A) Endogenous PL2L60 is dominantly detected in nuclear granules called nuage in MDA-MB-231 cells and co-localizes with stable expressed GFP-tagged LC3, both of which are established nuage components in the nucleus. (B) Perinuclear basal GFP-LC3B puncta (arrow) formation in stable transfected MDA-MB-231 cells. PL2L60, Piiwil2-like 60 kDa protein; LC3, microtubule-associated protein 1 light chain 3.

cells, which were transfected with siRNA E21, as demonstrated by flow cytometric analysis (Fig. 8C and D). Taken together, PL2L60 silencing could inhibit tumor growth through inducing apoptosis in cancer cells. To verify the *in vitro* results, PL2L60 was examined expression in tumor cell-derived xenografts.

**Hypoxia-induced necroptosis of cancers is a primary site for autophagic cell death and PL2L60 degradation.** Since oxygen diffusion distance is no more than 200 microns away from a capillary (41), cancer cells encounter hypoxic stress at a very early stage during cancer development. Most research have verified that hypoxia is the primary site for autophagy in tumors and induces autophagic cell death in cancer cells (20,28,42,43). Especially, it has been previously reported by the authors that autophagy can mediate programmed cell death (PCD) of breast and cervical cancer cells in responding to CoCl<sub>2</sub> mimic hypoxia (28). To determine whether a similar situation exists in hypoxic tumor regions *in vivo*, the prevalence and distribution of HIF-1 $\alpha$ , LC3, p62, PL2L60 and cleaved-caspase 3 was assessed in the MDA-MB-231 and HeLa-derived xenotransplant tumors. It was found that autophagy, as evaluated by positive expression of LC3B and downregulated expression of p62, was more strongly associated with hypoxic tumor regions than non-hypoxia (proliferating) tumor regions (Fig. 9). Conversely, both HIF-1 $\alpha$  and PL2L60 expression decreased significantly in the nested hypoxic tumor area compared with the normal adjacent proliferating area (Fig. 9). A previous study reported that the activation of autophagy under hypoxia decreases the amount of HIF-1 $\alpha$  via LC3 dependent manner in the presence of an intact autophagic machinery (23). This could explain the downregulation of HIF-1 $\alpha$  in the hypoxic tumor region. In line with the present western blot results (Figs. 2-7), PL2L60 was high in the normal adjacent proliferating area and low in the nested hypoxic tumor area (Fig. 9). Collectively, hypoxia-induced autophagy significantly decreased PL2L60 expression



*in vivo* or *in vitro*. In previous studies, it was confirmed that PL2L60 promotes tumor cell survival and proliferation (Fig. 9A and B) and severe hypoxia induces autophagy dependent PCD in cancer cells by activating caspase-3 (2,28). Autophagy can promote cell death by selectively reducing the abundance of anti-apoptotic proteins in the cells (44). Therefore, it was hypothesized that hypoxia would promote autophagic degradation of PL2L60 as one cancer cell death mechanism *in vivo*. IHC using an antibody against Ki67, a marker of cell proliferation, showed that Ki67-positive cells were decreased in severe hypoxic areas as compared with the normal adjacent proliferation area (Fig. 9), demonstrating decreased cell proliferation induced by hypoxia. H&E staining demonstrated more dead cells and the evident increase in apoptosis proportion in severe hypoxic tumor tissues (Fig. 9). IHC also demonstrated the increase in mean areas that stained positively for cleaved caspase-3 in severe hypoxic tumor tissues (Fig. 9). Collectively, the results revealed that hypoxia-induced autophagy inhibits growth and promotes apoptosis of breast or cervical cancer cells *in vivo* with lower levels of PL2L60, which may serve as an indicator for predicting clinical outcomes of cancer patients.

## Discussion

Solid tumor is always confronting the highly hypoxic, nutrient-poor environment, which may be a major cause of cancer cell death. However, the mechanisms underlying the metabolic stresses-induced cancer cell death remain elusive. In the present study, it was identified for the first time, to the best of our knowledge, that the cancer cell death induced by hypoxia and nutrient deprivation was associated with autophagic degradation of PL2L60 in various types of cancer cells (Figs. 1-9). The hypoxia-induced PL2L60 downregulation was independent of HIF-1 $\alpha$ , which is a key molecule in the regulation of oxygen homeostasis (Fig. 3). Cells exposed to various stressors undergo a process of self-digestion known as autophagy, during which cytoplasmic or nuclear cargo sequestered inside double-membrane vesicles are delivered to the lysosome for degradation. Consistently, inhibition of autophagy by targeting Beclin-1 (*BECN1*) or ATG5 restored PL2L60 levels in the hypoxic cancer cells *in vitro* (Fig. 5A and B). Accordingly, knockdown of the autophagosome membrane protein Atg8/LC3 or autophagy cargo protein p62 by siRNA attenuated the hypoxia-induced degradation of PL2L60 (Fig. 5C-F). Cytological analysis confirmed existence of LC3/PL2L60 punctate complexes in the cancer cells (Figs. 6 and 7). These findings indicated that metabolic stress-induced cancer cell death was associated with the selective autophagosomal clearance of PL2L60.

In a solid cancer, necroptosis is frequently observed, which may be caused by reduced oxygen tension (hypoxia) within the tumor (17,20,30). The reduced oxygen tensions may induce HIF-1 $\alpha$ , which plays an essential role in homeostatic response to the hypoxia, activating the transcription of over 40 genes including erythropoietin, glucose transporters, glycolytic enzymes, vascular endothelial growth factor and other genes (17,20,30,31). The protein products of these genes increase oxygen delivery or facilitate metabolic adaptation

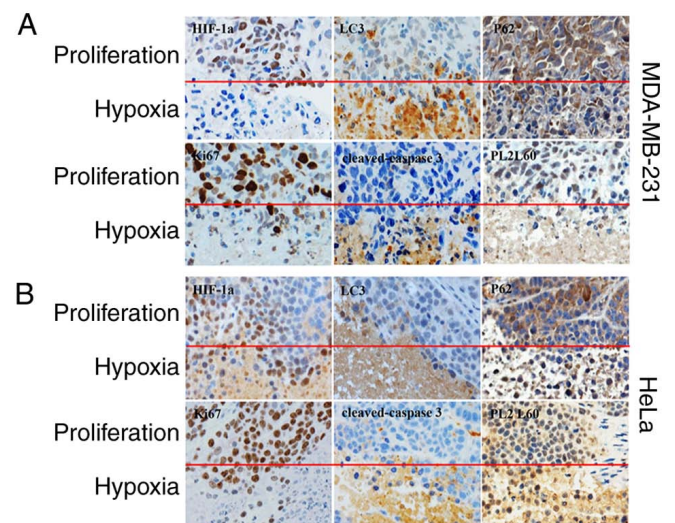


Figure 9. Loss of PL2L60 suppresses proliferation and promotes tumor autophagic cell death in nude mice under hypoxia. (A and B) Representative images of immune histochemical staining using antibodies (anti-HIF-1 $\alpha$ , anti-LC3, anti-p62, anti-PL2L60, anti-cleaved caspase 3 and anti-Ki67) against the indicated proteins in severe hypoxic tumor areas (Hypoxia) and non-hypoxia tumor proliferating areas (Proliferation) of (A) breast or (B) HeLa cancer tissues from one wild-type mouse. H&E staining was used to evaluate the histology. Magnification, x40.

to hypoxia. This means that in addition to protective role of HIF-1 $\alpha$ , there should be a pathway that antagonizes the role of HIF-1 $\alpha$  to drive the oxygen-deficient cancer cells to apoptotic death. In the present study, it was identified that such a pathway of autophagic degradation of PL2L60 proteins was independent of HIF-1 $\alpha$ .

In cancer cells, autophagy is a double sword, which can be neutral, tumor-suppressive, or tumor-promoting in different contexts. It has mainly been considered that autophagy can promote cancer through suppressing p53 and preventing energy crisis, cell death, senescence, and an antitumor immune response (45). In the present study, however, it was demonstrated that in the hypoxia or nutrient-deprivation context, activating autophagy induced apoptosis of cancer cells through selectively degradation of PL2L60, a key promoter of cancer cell survival and proliferation (2,4-6). This finding was consistent with the conclusion that PL2L60 is a tumorigenic promoter (2-5), and blocking PL2L60 could suppress tumor growth.

While autophagosomes sequester cytosolic materials non-specifically in a process called non-selective autophagy, a process of selective autophagy also occurs in which autophagic degradation of specific protein aggregates or organelles targeted for destruction occurs (32,46). A previous study has reported that LC3 can co-operates with p62 to deliver mitochondrial proteins to lysosomes for selective degradation (47). Selective autophagy degrading specific proteins is often associated with degradation of p62 or NDP52, a protein complex that binds ubiquitinated protein aggregates and LC3 family protein to target them for degradation (47-50). Knockdown of p62 reversed the hypoxic degradation of PL2L60, suggesting that PL2L60 may be specifically or selectively degraded by autophagy in the contexts of metabolic stresses. LC3-PL2L60 interaction alone without p62 was not sufficient for PL2L60

degradation (Fig. 5C-F), suggesting that PL2L60 was selectively degraded in the hypoxic environment.

PL2L60 is a truncated protein of PIWIL2, containing ½ PAZ domain and a PIWI domain (2). Piwi interacts with polycomb group complexes PRC1 and PRC2 in niche and germline cells to regulate ovarian, germline stem cells and oogenesis (51). The Mili (Piwil2)-containing complexes (sometimes named pi-body) can be isolated from adult mouse testes, which contain some key proteins such as Tudor domain-containing protein-1 or 12 (Tdrd1/12) and play a vital role in piRNA biogenesis and maturity in the cytoplasm (52-54). Indeed, it was observed that PL2L60 speckles accumulated in the cancer nucleus (Figs. 6 and 7). Although both LC3 and p62 plays the key role in the PL2L60 degradation (Figs. 4 and 5), how PL2L60 as one autophagic substrate was sequestered in the nucleus and then transferred into the cytoplasm for autophagic degradation yet remained unclear. As shown in Fig. 6, PL2L60 is distributed dominantly in the nucleus and fewer puncta scattered in the cytoplasm. Nuclear autophagy is evolutionarily conserved in eukaryotes that may target various nuclear components through a series of processes, including nuclear sensing, nuclear export, autophagic substrate encapsulation and autophagic degradation in the cytoplasm (55,56). For instance, nuclear lamina protein Lamin B1 degradation is achieved by nucleus-to-cytoplasm transport that delivers Lamin B1 to the lysosome (56). It was also observed that GFP puncta predominantly distributed in the perinuclear (Fig. 7B). Importantly, merging LC3 and PL2L60 fluorescence revealed a nuclear co-localization for these two proteins while PL2L60 could not be detected in the GFP-LC3 puncta positive autophagosomes-like structures (Fig. 7A and B). Therefore, the predominant perinuclear distribution of lysosomes (57) may facilitate this cargo and degradation of PL2L60.

Symmetrical dimethylarginines (sDMA) modification is required for Piwi protein stability favoring piRNA biogenesis (58). Most animal Piwi proteins contain sDMA motifs that are typically clustered close to the amino terminus (58). Protein post-translational modification provides a layer of regulation for the specificity and efficiency of selective autophagy (48,50). In a previous by the authors, it was confirmed that asymmetric DMA (aDMA) serves as one specific degradation signal of selective autophagy (59). Especially, a previous study found that arginine methylation regulates the autophagic degradation efficiency of PGL Granules [PGL-1 and PGL-3 (cargo)-SEPA-1 (receptor) complexes] (60). In the present study, some autophagosomal structures containing PL2L60 were observed to dominantly express in the nucleus and partly in the perinucleus (Fig. 6A). Moreover, GFP-LC3 and PL2L60 accumulated in the nucleus and interacted with each other (Fig. 7A). Subsequent studies should evaluate the relative sDMA or aDMA potential of PL2L60 and assess other regions of their cytoplasmic or nuclear domain sequences for the involvement in PL2L60 degradation.

The present results indicated that hypoxia-regulated autophagy induced apoptosis in multiple types of cancer by suppressing PL2L60. The present study has established an intimate relationship between autophagy, PL2L60 and apoptosis in response to hypoxia. The present study may provide rational

strategies for the future clinical evaluation of PL2L60 as one key cancer immunotherapy antigen in targeted molecular strategy.

### Acknowledgements

The authors are grateful to Dr Yanfeng Liu (Renji-Med X Clinical Stem Cell Research Center, Ren Ji Hospital) for his stimulating discussion and helpful comments on the manuscript.

### Funding

The present study was supported by the SJTU Interdisciplinary Research Grant (grant no. YG2015MS56), the National Natural Science Foundation of China (grant nos. 81402287, 81602700, 81672713, 81372188, and 81371507), the Science and technology support program, Science and Technology Commission of Shanghai Municipality (grant no. 1243190074), The Special Fund for Innovation and Development of Science and Technology and Cultivation Fund for Major Projects and Innovative Team, the Shanghai Jiao Tong University, the State Key Laboratory of Oncogenes and Related Genes in China (grant no. 90-14-06), the Startup Funds from Renji Hospital and School of Medicine, Shanghai Jiao Tong University and the Fund for Key Disciplines and Specialties, Shanghai Health and Family Planning Committee.

### Availability of data and materials

The datasets used and/or analyzed during the current study are available from the corresponding author on reasonable request.

### Authors' contributions

LS, LFL and JXG conceived the project and supervised the study. LS, FH and GYT initiated the project and performed the experiments. HLS conducted part of the experiments. LS, XLC and LFL analyzed and interpreted the data. LS and LFL designed the experiments and drafted the manuscript. All authors read and approved the final version of the manuscript. LS, LFL and JXG confirm the authenticity of all the raw data.

### Ethics approval and consent to participate

Nude mice were obtained from SLACCAS (Shanghai Laboratory Animal Center), bred in our own animal pathogen-free facility and maintained under standard conditions according to the institutional guidelines of Renji Hospital animal care and ethics review committee. All *in vivo* experiments were approved by the institutional guidelines of the animal care and ethics review committee of Renji Hospital (Shanghai, China).

### Patient consent for publication

Not applicable.

### Competing interests

The authors declare that they have no competing interests.

## References

- Chen L, Shen R, Ye Y, Pu XA, Liu X, Duan W, Wen J, Zimmerer J, Wang Y, Liu Y, *et al*: Precancerous stem cells have the potential for both benign and malignant differentiation. *PLoS One* 2: e293, 2007.
- Ye Y, Yin DT, Chen L, Zhou Q, Shen R, He G, Yan Q, Tong Z, Issekutz AC, Shapiro CL, *et al*: Identification of Piwil2-like (PL2L) proteins that promote tumorigenesis. *PLoS One* 5: e13406, 2010.
- Gainetdinov IV, Skvortsova YV, Stukacheva EA, Bychenko OS, Kondratieva SA, Zinovieva MV and Azhikina TL: Expression profiles of PIWIL2 short isoforms differ in testicular germ cell tumors of various differentiation subtypes. *PLoS One* 9: e112528, 2014.
- Liu SS, Liu N, Liu MY, Sun L, Xia WY, Lu HM, Fu YJ, Yang GL, Bo JJ, Liu XX, *et al*: An unusual intragenic promoter of PIWIL2 contributes to aberrant activation of oncogenic PL2L60. *Oncotarget* 8: 46104-46120, 2017.
- Li LF, Liu N, Liu MY and Gao JX: The Functions of Piwil2 and Its Prospects in Tumorigenesis. *Am J Transl Med* 1: 75-98, 2017.
- Gao JX, Liu N and Wu HL: PIWIL2 (piwi-like RNA-mediated gene silencing 2). *Atlas Genet Cytogenet Oncol Haematol* 18: 919-927, 2014.
- Czech B and Hannon GJ: Small RNA sorting: Matchmaking for Argonautes. *Nat Rev Genet* 12: 19-31, 2011.
- Yang Z, Chen KM, Pandey RR, Homolka D, Reuter M, Janeiro BK, Sachidanandam R, Fauvarque MO, McCarthy AA and Pillai RS: PIWI slicing and EXD1 drive biogenesis of nuclear piRNAs from cytosolic targets of the mouse piRNA pathway. *Mol Cell* 61: 138-152, 2016.
- Vourekas A and Mourelatos Z: HITS-CLIP (CLIP-Seq) for mouse Piwi proteins. *Methods Mol Biol* 1093: 73-95, 2014.
- Vourekas A, Alexiou P, Vrettos N, Maragkakis M and Mourelatos Z: Sequence-dependent but not sequence-specific piRNA adhesion traps mRNAs to the germ plasm. *Nature* 531: 390-394, 2016.
- Hirakata S and Siomi MC: piRNA biogenesis in the germline: From transcription of piRNA genomic sources to piRNA maturation. *Biochim Biophys Acta* 1859: 82-92, 2016.
- Yin DT, Wang Q, Chen L, Liu MY, Han C, Yan Q, Shen R, He G, Duan W, Li JJ, *et al*: Germline stem cell gene PIWIL2 mediates DNA repair through relaxation of chromatin. *PLoS One* 6: e27154, 2011.
- Kim E, Goren A and Ast G: Alternative splicing: Current perspectives. *Bioessays* 30: 38-47, 2008.
- Xin D, Hu L and Kong X: Alternative promoters influence alternative splicing at the genomic level. *PLoS One* 3: e2377, 2008.
- Yang X, Coulombe-Huntington J, Kang S, Sheynkman GM, Hao T, Richardson A, Sun S, Yang F, Shen YA, Murray RR, *et al*: Widespread expansion of protein interaction capabilities by alternative splicing. *Cell* 164: 805-817, 2016.
- Thadani-Mulero M, Portella L, Sun S, Sung M, Matov A, Vessella RL, Corey E, Nanus DM, Plymate SR and Giannakakou P: Androgen receptor splice variants determine taxane sensitivity in prostate cancer. *Cancer Res* 74: 2270-2282, 2014.
- Vaupel P, Kelleher DK and Höckel M: Oxygen status of malignant tumors: Pathogenesis of hypoxia and significance for tumor therapy. *Semin Oncol* 28 (2 Suppl 8): S29-S35, 2001.
- Ueda S, Saeki T, Osaki A, Yamane T and Kuji I: Bevacizumab induces acute hypoxia and cancer progression in patients with refractory breast cancer: Multimodal functional imaging and multiplex cytokine analysis. *Clin Cancer Res* 23: 5769-5778, 2017.
- Sun L, Li T, Wei Q, Zhang Y, Jia X, Wan Z and Han L: Upregulation of BNIP3 mediated by ERK/HIF-1 $\alpha$  pathway induces autophagy and contributes to anoxic resistance of hepatocellular carcinoma cells. *Future Oncol* 10: 1387-1398, 2014.
- Azad MB, Chen Y, Henson ES, Cizeau J, McMillan-Ward E, Israels SJ and Gibson SB: Hypoxia induces autophagic cell death in apoptosis-competent cells through a mechanism involving BNIP3. *Autophagy* 4: 195-204, 2008.
- Luo J, Solimini NL and Elledge SJ: Principles of cancer therapy: Oncogene and non-oncogene addiction. *Cell* 136: 823-837, 2009.
- Klionsky DJ and Emr SD: Autophagy as a regulated pathway of cellular degradation. *Science* 290: 1717-1721, 2000.
- Bellot G, Garcia-Medina R, Gounon P, Chiche J, Roux D, Pouyssegur J and Mazure NM: Hypoxia-induced autophagy is mediated through hypoxia-inducible factor induction of BNIP3 and BNIP3L via their BH3 domains. *Mol Cell Biol* 29: 2570-2581, 2009.
- Xie Z and Klionsky DJ: Autophagosome formation: Core machinery and adaptations. *Nat Cell Biol* 9: 1102-1109, 2007.
- Tsujimoto Y and Shimizu S: Another way to die: Autophagic programmed cell death. *Cell Death Differ* 12 (Suppl 2): S1528-S1534, 2005.
- Gewirtz DA: The four faces of autophagy: Implications for cancer therapy. *Cancer Res* 74: 647-651, 2014.
- Song J, Guo X, Xie X, Zhao X, Li D, Deng W, Song Y, Shen F, Wu M and Wei L: Autophagy in hypoxia protects cancer cells against apoptosis induced by nutrient deprivation through a Beclin1-dependent way in hepatocellular carcinoma. *J Cell Biochem* 112: 3406-3420, 2011.
- Sun L, Liu N, Liu SS, Xia WY, Liu MY, Li LF and Gao JX: Beclin-1-independent autophagy mediates programmed cancer cell death through interplays with endoplasmic reticulum and/or mitochondria in colbat chloride-induced hypoxia. *Am J Cancer Res* 5: 2626-2642, 2015.
- Philip B, Ito K, Moreno-Sánchez R and Ralph SJ: HIF expression and the role of hypoxic microenvironments within primary tumours as protective sites driving cancer stem cell renewal and metastatic progression. *Carcinogenesis* 34: 1699-1707, 2013.
- Majmudar AJ, Wong WJ and Simon MC: Hypoxia-inducible factors and the response to hypoxic stress. *Mol Cell* 40: 294-309, 2010.
- Ivan M, Kondo K, Yang H, Kim W, Valiando J, Ohh M, Salic A, Asara JM, Lane WS and Kaelin WG Jr: HIF $\alpha$  targeted for VHL-mediated destruction by proline hydroxylation: Implications for O<sub>2</sub> sensing. *Science* 292: 464-468, 2001.
- Kristensen AR, Schandorff S, Høyer-Hansen M, Nielsen MO, Jäättelä M, Dengjel J and Andersen JS: Ordered organelle degradation during starvation-induced autophagy. *Mol Cell Proteomics* 7: 2419-2428, 2008.
- Li HY, Zhang J, Sun LL, Li BH, Gao HL, Xie T, Zhang N and Ye ZM: Celastrol induces apoptosis and autophagy via the ROS/JNK signaling pathway in human osteosarcoma cells: An in vitro and in vivo study. *Cell Death Dis* 6: e1604, 2015.
- Maiuri MC, Zalckvar E, Kimchi A and Kroemer G: Self-eating and self-killing: Crosstalk between autophagy and apoptosis. *Nat Rev Mol Cell Biol* 8: 741-752, 2007.
- Liang XH, Jackson S, Seaman M, Brown K, Kempkes B, Hibshoosh H and Levine B: Induction of autophagy and inhibition of tumorigenesis by beclin 1. *Nature* 402: 672-676, 1999.
- Liang C, Feng P, Ku B, Dotan I, Canaani D, Oh BH and Jung JU: Autophagic and tumour suppressor activity of a novel Beclin1-binding protein UVRAG. *Nat Cell Biol* 8: 688-699, 2006.
- Johansen T and Lamark T: Selective autophagy mediated by autophagic adapter proteins. *Autophagy* 7: 279-296, 2011.
- Kobayashi H and Tomari Y: RISC assembly: Coordination between small RNAs and Argonaute proteins. *Biochim Biophys Acta* 1859: 71-81, 2016.
- Da Ros M, Lehtiniemi T, Olotu O, Fischer D, Zhang FP, Vihinen H, Jokitalo E, Sironen A, Toppari J and Kotaja N: FYCO1 and autophagy control the integrity of the haploid male germ cell-specific RNP granules. *Autophagy* 13: 302-321, 2017.
- Link S, Grund SE and Diederichs S: Alternative splicing affects the subcellular localization of Drosha. *Nucleic acids research* 44: 5330-5343, 2016.
- Olive PL, Vikse C and Trotter MJ: Measurement of oxygen diffusion distance in tumor cubes using a fluorescent hypoxia probe. *Int J Radiat Oncol Biol Phys* 22: 397-402, 1992.
- Shimizu S, Eguchi Y, Kamiike W, Itoh Y, Hasegawa J, Yamabe K, Otsuki Y, Matsuda H and Tsujimoto Y: Induction of apoptosis as well as necrosis by hypoxia and predominant prevention of apoptosis by Bcl-2 and Bcl-XL. *Cancer Res* 56: 2161-2166, 1996.
- Rouschop KM, van den Beucken T, Dubois L, Niessen H, Bussink J, Savelkoul K, Keulers T, Mujcic H, Landuyt W, Voncken JW, *et al*: The unfolded protein response protects human tumor cells during hypoxia through regulation of the autophagy genes MAP1LC3B and ATG5. *J Clin Invest* 120: 127-141, 2010.
- Mariño G, Niso-Santano M, Baehrecke EH and Kroemer G: Self-consumption: The interplay of autophagy and apoptosis. *Nat Rev Mol Cell Biol* 15: 81-94, 2014.
- Amaravadi R, Kimmelman AC and White E: Recent insights into the function of autophagy in cancer. *Genes Dev* 30: 1913-1930, 2016.

46. Goodwin JM, Dowdle WE, DeJesus R, Wang Z, Bergman P, Kobylarz M, Lindeman A, Xavier RJ, McAllister G, Nyfeler B, *et al.*: Autophagy-independent lysosomal targeting regulated by ULK1/2-FIP200 and ATG9. *Cell Rep* 20: 2341-2356, 2017.
47. Le Guerroué F, Eck F, Jung J, Starzetz T, Mittelbronn M, Kaulich M and Behrends C: Autophagosomal content profiling reveals an LC3C-dependent piecemeal mitophagy pathway. *Mol Cell* 68: 786-796.e6, 2017.
48. Wild P, Farhan H, McEwan DG, Wagner S, Rogov VV, Brady NR, Richter B, Korac J, Waidmann O, Choudhary C, *et al.*: Phosphorylation of the autophagy receptor optineurin restricts Salmonella growth. *Science* 333: 228-233, 2011.
49. Newman AC, Kemp AJ, Drabsch Y, Behrends C and Wilkinson S: Autophagy acts through TRAF3 and RELB to regulate gene expression via antagonism of SMAD proteins. *Nat Commun* 8: 1537, 2017.
50. Jo C, Gundemir S, Pritchard S, Jin YN, Rahman I and Johnson GVW: Nrf2 reduces levels of phosphorylated tau protein by inducing autophagy adaptor protein NDP52. *Nat Commun* 5: 3496, 2014.
51. Peng JC, Valouev A, Liu N and Lin H: Piwi maintains germline stem cells and oogenesis in *Drosophila* through negative regulation of Polycomb group proteins. *Nat Genet* 48: 283-291, 2016.
52. Reuter M, Chuma S, Tanaka T, Franz T, Stark A and Pillai RS: Loss of the Mili-interacting Tudor domain-containing protein-1 activates transposons and alters the Mili-associated small RNA profile. *Nat Struct Mol Biol* 16: 639-646, 2009.
53. Aravin AA, van der Heijden GW, Castaneda J, Vagin VV, Hannon GJ and Bortvin A: Cytoplasmic compartmentalization of the fetal piRNA pathway in mice. *PLoS Genet* 5: e1000764, 2009.
54. Mathioudakis N, Palencia A, Kadlec J, Round A, Tripsianes K, Sattler M, Pillai RS and Cusack S: The multiple Tudor domain-containing protein TDRD1 is a molecular scaffold for mouse Piwi proteins and piRNA biogenesis factors. *RNA* 18: 2056-2072, 2012.
55. Luo M, Zhao X, Song Y, Cheng H and Zhou R: Nuclear autophagy: An evolutionarily conserved mechanism of nuclear degradation in the cytoplasm. *Autophagy* 12: 1973-1983, 2016.
56. Dou Z, Xu C, Donahue G, Shimi T, Pan JA, Zhu J, Ivanov A, Capell BC, Drake AM, Shah PP, *et al.*: Autophagy mediates degradation of nuclear lamina. *Nature* 527: 105-109, 2015.
57. Tan KP, Ho MY, Cho HC, Yu J, Hung JT and Yu AL: Fucosylation of LAMP-1 and LAMP-2 by FUT1 correlates with lysosomal positioning and autophagic flux of breast cancer cells. *Cell Death Dis* 7: e2347, 2016.
58. Kirino Y, Kim N, de Planell-Saguer M, Khandros E, Chiorean S, Klein PS, Rigoutsos I, Jongens TA and Mourelatos Z: Arginine methylation of Piwi proteins catalysed by dPRMT5 is required for Ago3 and Aub stability. *Nat Cell Biol* 11: 652-658, 2009.
59. Sun L, Xia WY, Zhao SH, Liu N, Liu SS, Xiu P, Li LF, Cao XL and Gao JX: An asymmetrically dimethylarginated nuclear 90 kDa protein (p90aDMA) induced by interleukin (IL)-2, IL-4 or IL-6 in the tumor microenvironment is selectively degraded by autophagy. *Int J Oncol* 48: 2461-2471, 2016.
60. Li S, Yang P, Tian E and Zhang H: Arginine methylation modulates autophagic degradation of PGL granules in *C. elegans*. *Mol Cell* 52: 421-433, 2013. *Ritio optatur sinvelignis ut arum que lanturerum il et, quatio. Nam et et escia audi aciis nia idis eum hilit volor molorat.*



Copyright © 2024 Sun *et al.* This work is licensed under a Creative Commons Attribution-NonCommercial-NoDerivatives 4.0 International (CC BY-NC-ND 4.0) License.